

Yang, and C. P. Yang, *ibid.* **19**, 588 (1967).

<sup>5</sup>F. Y. Wu, Phys. Rev. Letters **18**, 605 (1967).

<sup>6</sup>F. Y. Wu, Phys. Rev. **168**, 539 (1968).

<sup>7</sup>F. Y. Wu, Phys. Rev. **183**, 604 (1969).

<sup>8</sup>F. Y. Wu, Phys. Rev. Letters **22**, 1174 (1969).

<sup>9</sup>C. Fan and F. Y. Wu, Phys. Rev. **179**, 560 (1969).

<sup>10</sup>The symmetry relations (7a) have been obtained in Ref. 9.

<sup>11</sup>J. F. Nagle, J. Math. Phys. **9**, 1007 (1968).

<sup>12</sup>Discussion in Ref. 7 was specialized to the case  $u_3 = 1$ ,  $u_4 = u_1 u_2$ . The derivation of (12) and (14) presents no problem if one follows the procedures of Ref. 7 and uses the notations  $u_3$  and  $u_4$  in places of 1 and  $u_1 u_2$ .

<sup>13</sup>E. H. Lieb, Phys. Rev. Letters **18**, 692 (1967).

<sup>14</sup>Except the  $F$  model for which the specific heat is continuous at  $T_c$ . But this has been identified in Ref. 8 as a limiting situation of the more familiar  $\lambda$  transitions.

<sup>15</sup>See the Appendix of Ref. 7.

<sup>16</sup>In the discussion of the general planar Ising models, Hurst and Green [H. S. Green and C. A. Hurst, in *Order-Disorder Phenomena*, edited by I. Preigoiné (Interscience, New York, 1964), Sec. 5.3] have considered the same problem from a somewhat different point of

view. They considered the simple quartic Ising lattice and introduced at each vertex point a sublattice to generate what is equivalent to our vertex weights. It can be shown that the free-fermion condition (15) is always an identity in their considerations provided that the sublattice introduced at each vertex is planar. The condition (15) therefore also reflects the solubility of planar Ising lattices.

<sup>17</sup>Green and Hurst (Ref. 15) have evaluated some derivatives of the partition function (16). Our discussions are simpler because of the special form of the vertex weights (2) and the use of relation (19).

<sup>18</sup>J. Stephenson, Can J. Phys. **47**, 2621 (1969).

<sup>19</sup>J. Stephenson, J. Math. Phys. **11**, 420 (1970).

<sup>20</sup>That the present model is identical to the modified  $F$  model (MF) is proved in the Appendix of Ref. 7.

<sup>21</sup>See, for example, E. W. Montroll, in *Applied Combinatorial Mathematics*, edited by E. F. Beckenbach (Wiley, New York, 1964), Chap. 4.

<sup>22</sup>The usefulness of this dimer city has also been observed by M. E. Fisher (private communication).

<sup>23</sup>Except with the replacement of  $b$ ,  $c$  by  $-b$ ,  $-c$  in (16). But these are equivalent expressions.

## Elastic Properties of $\text{MnF}_2$ †

R. L. Melcher\*

*Laboratory of Atomic and Solid State Physics, Cornell University, Ithaca, New York 14850*

(Received 9 February 1970)

The elastic properties of  $\text{MnF}_2$  have been investigated in the temperature range  $4.2 < T < 330$  K using a cw transmission technique. The measured values at  $T = 300$  K of the six adiabatic elastic constants in units of  $10^{11}$  dyn/cm<sup>2</sup> are  $c_{11} = 10.24$ ,  $c_{33} = 16.55$ ,  $c_{44} = 3.185$ ,  $c_{66} = 7.208$ ,  $c_{12} = 7.95$ , and  $c_{13} = 7.07$ . The elastic Debye temperature calculated from the low-temperature elastic-constant data is  $\Theta_D(E) = 261.6$  K. Using the force-constant model of Matossi for the rutile structure and the published frequencies of the Raman-active vibrational modes, theoretical values of the elastic constants are calculated and found to be in fair agreement with experiment. Each elastic constant [except  $c' = \frac{1}{2}(c_{11} - c_{12})$ ] shows the expected linear decrease with increasing temperature in the region  $T \gtrsim \Theta_D(E)$ . On the other hand,  $c'$  has not yet reached this limiting high-temperature behavior at  $T = 330$  K. The effects on the elastic properties of volume magnetostrictive coupling to the spin fluctuations near the Néel temperature ( $T \approx T_N$ ) and of linear magneto-elastic coupling to the magnetic modes in the antiferromagnetic state ( $T < T_N$ ) are discussed. The elastic constant  $c_{44}$  is found to have a component at low temperatures ( $T < T_N$ ) decreasing approximately as  $T^{-1}$ . This striking phenomenon is discussed on the basis of two possible processes, neither of which provides a completely satisfactory explanation.

### I. INTRODUCTION

The study of the propagation of ultrasonic waves in antiferromagnetically ordered media has proven to be a valuable tool for the investigation of a variety of phenomena. Velocity measurements are used to measure the elastic<sup>1,2</sup> and magneto-elastic coupling constants,<sup>3,4</sup> attenuation and velocity measurements are used to study dynamic critical phenomena in the neighborhood of the Néel temperature<sup>5</sup>; anomalies in the elastic properties at the spin-flop transition have been used to study the magnetic phase diagram<sup>6</sup>; and finally, it has

been shown that in certain systems resonant nuclear spin-phonon interactions can be studied.<sup>7,8</sup>

In this paper, a systematic study of the elastic properties of  $\text{MnF}_2$  is reported. The adiabatic elastic constants associated with longitudinal and transverse ultrasonic propagation along each of the symmetry directions [001], [110], and [100], as well as the nonsymmetry direction perpendicular to the (011) plane have been measured in the temperature region from 4.2 to 330 K. These measurements provide a complete description of the elastic properties of this material.

$\text{MnF}_2$  is an attractive material in which to study

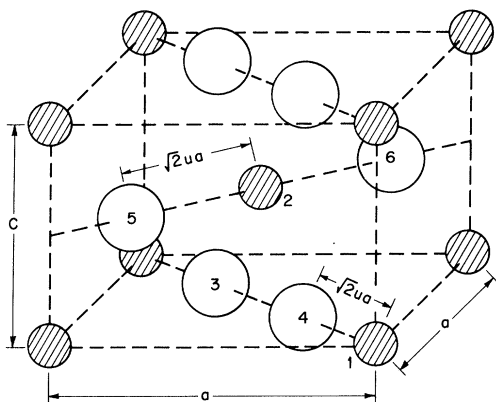


FIG. 1. Rutile structure of  $\text{MnF}_2$  showing the six atoms of a unit cell. The solid circles are  $\text{Mn}^{2+}$  ions and the open circles are  $\text{F}^-$  ions.

the elastic properties for several reasons. It crystallizes with rutile structure (space group  $D_{4h}^{14} - P4/mnm$ ). The tetragonal unit cell (see Fig. 1) containing two  $\text{MnF}_2$  molecules has "c" and "a" axis dimensions of  $3.3103 \pm 0.001 \text{ \AA}$  and  $4.8734 \pm 0.0005 \text{ \AA}$ , respectively, at 298 K. The density (also at  $T = 298 \text{ K}$ ) is  $3.922 \pm 0.004 \text{ g/cm}^3$ . Each  $\text{Mn}^{2+}$  ion is surrounded by a distorted octahedron of  $\text{F}^-$  ions. The quantity  $u$  which determines the positions of the  $\text{F}^-$  ions has the value  $0.310 \pm 0.005$ . The angle 3-2-4 (see Fig. 1) has the value  $76.7^\circ$ . The distance between atoms 2 and 5 (Fig. 1) is  $2.14 \text{ \AA}$ , while that between 2 and 4 is  $2.11 \text{ \AA}$ .<sup>9</sup>

The magnetic properties of  $\text{MnF}_2$  have been extensively studied by a variety of techniques and are believed to be relatively well understood. Below its Néel temperature ( $T_N = 67.3 \text{ K}$ )  $\text{MnF}_2$  is known to order antiferromagnetically in a simple two sublattice configuration. The c, or [001] axis, is the axis of easy magnetization. The vibrational spectrum and elastic properties of materials with the rutile structure have been of considerable interest in recent years and have been studied extensively using Raman scattering, infrared spectroscopy, and ultrasonic methods.<sup>10-16</sup>

In Sec. II, the samples and the experimental techniques used in the present work are described. Section III is devoted to a presentation of the experimental results which are discussed later in Sec. IV.

## II. EXPERIMENTAL

### A. Samples and Their Preparation

The two single-crystal samples of  $\text{MnF}_2$  (designated 01 and 02) used in the present experiments were approximately in the form of cubes 1 cm on a side.<sup>17</sup> They were of high optical quality. Chemical analysis showed the following impurity content: 0.1–1 ppm of Cr, V,

Co, Ni; 1–10 ppm of Ca, Mg, Al, Cu, Na, K; 10–100 ppm of Fe, Si.

The samples were oriented using Bragg angle diffraction x-ray techniques to  $\pm 0.15^\circ$  of the desired orientation. Two pairs of surfaces on each sample were then polished flat and parallel to better than  $\pm 5 \times 10^{-5} \text{ cm}$  using  $\text{Al}_2\text{O}_3$  grit on glass with a 1:1 mixture of  $\text{H}_2\text{O}$  and glycerin serving as carrier.

### B. Temperature Measurement and Control

The crystals and temperature sensors were mounted in good thermal contact with a copper holder. The temperature of the holder was maintained constant (typically to  $\pm 0.05 \text{ K}$ ) with a servo-regulated controller (Artronix Model 5301). Calibrated germanium (Cryocal CR1000) and platinum (Rosemont #118L) resistance thermometers were used for the temperature measurements.

### C. Ultrasonic Velocity Measurements

The transmission-type frequency-modulation technique used in the present study for the measurement of ultrasonic phase velocities has been described elsewhere.<sup>18</sup> The measurements reported here were all carried out at a frequency  $\nu \approx 30 \text{ MHz}$ .

Longitudinal and transverse ultrasonic waves were generated and received using resonant X- and AC-cut natural quartz transducers which were bonded to the sample with stopcock grease or silicone transistor grease. The silicone grease provided a more reliable bond at low temperatures.

The thermal expansion data of Gibbons<sup>19</sup> were used to correct for sample length and density changes.

The absolute accuracy of the velocity measurement is about  $\pm 1\%$ . Each measurement was checked at room temperature using the cw method at both 10 and 30 MHz and with a simple pulse-echo technique at 30 MHz.

### D. Calculation of Elastic Constants

The elastic free-energy density of a crystal belonging to the  $D_{4h}^{14} - P4/mnm$  space group can be written in terms of six elastic constants  $c_{ij}$  and the elastic strains  $e_{ij}$  as

$$E = \frac{1}{2} c_{11} (e_{xx}^2 + e_{yy}^2) + \frac{1}{2} c_{33} e_{zz}^2 + \frac{1}{2} c_{44} (e_{xz}^2 + e_{yz}^2) + \frac{1}{2} c_{66} e_{xy}^2 + c_{12} e_{xx} e_{yy} + c_{13} (e_{xx} e_{zz} + e_{yy} e_{zz}). \quad (1)$$

The strains are defined in terms of the elastic displacement field  $u_i(\vec{r}, t)$ ,  $i = x, y, z$ ,

$$e_{ij} = \left(1 - \frac{1}{2} \delta_{ij}\right) \left( \frac{\partial u_i}{\partial x_j} + \frac{\partial u_j}{\partial x_i} \right). \quad (2)$$

All of the elastic constants except  $c_{13}$  can be calculated from the measured phase velocity of pure transverse or pure longitudinal modes propagating

along the symmetry axes of the crystals. In order to calculate  $c_{13}$ , measurements must be made of the quasilongitudinal and/or quasitransverse modes obtained from off-axis propagation. The modes studied and the expressions used to calculate the elastic constants are summarized in Table I.

Elastic stability<sup>20</sup> requires that the elastic free-energy density [Eq. (1)] be a positive definite quadratic form in the strains  $e_{ij}$ . This imposes the conditions that  $c_{11}$ ,  $c_{33}$ ,  $c_{44}$ ,  $c_{66}$ ,  $c' = \frac{1}{2}(c_{11} - c_{12})$  and  $c \equiv c_{33}(c_{11} + c_{12}) - 2c_{13}^2$  are each positive. The latter condition must be used to eliminate an extraneous solution when calculating the value of  $c_{13}$  from the measured value of either  $c_{QL}$  or  $c_{QT}$  (see Table I).

### III. EXPERIMENTAL RESULTS

The values of the combination of elastic constants at four temperatures, obtained from each of the several elastic modes studied as well as the derived constants  $c_{12}$  and  $c_{13}$ , are summarized in Table II. The temperature coefficient of each mode at  $T = 300$  K defined as  $-(\partial/\partial T)[\ln c_{ij}]$  is also given along with the "athermal" values determined by linear extrapolation of the high-temperature data to  $T = 0$  K.<sup>21</sup> The temperature coefficient for  $c' = \frac{1}{2}(c_{11} - c_{12})$  is not given because the limiting high-temperature behavior has not been reached for this mode at  $T = 330$  K (Fig. 2). The elastic Debye

temperature  $\Theta_D(E)$  is also given at each temperature.

The absolute accuracy of the directly measured elastic constants is  $\pm 2\%$  while the derived constants  $c_{12}$  and  $c_{13}$  have an accuracy of  $\sim \pm 4\%$ . The significant figures retained in Table II refer to the relative precision of the data, which is considerably higher. Numerous internal consistency checks on the values of the elastic constants are possible from the measured values of the eleven modes given in Table I. Consistency was found in each case to be well within the quoted error.

The calculation of the elastic Debye temperature  $\Theta_D(E)$  from the measured values of the adiabatic elastic constants was performed using the tetragonal harmonic method of Betts *et al.*<sup>22</sup> By ignoring all harmonics of degree  $l = 8$  or higher, the accuracy of the calculation should be  $\approx 2\%$ .

The number density  $N/V$  was taken to be the number density of  $\text{MnF}_2$  molecules. The low-temperature value of  $\Theta_D(E) = 261.6 \pm 6.0$  K compares to the value  $\Theta_D = 253$  K obtained from low-temperature calorimetric measurements.<sup>23</sup>

The temperature dependence of the elastic modes for each propagation direction is presented in Figs. 2–5. In Fig. 6, the low-temperature behavior of  $c_{33}$  and  $c_{44}$  obtained from propagation along the  $[001]$  axis is shown in more detail. Measurements of  $c_{44}$  obtained from transverse propagation along the  $[110]$  and  $[100]$  axes (see

TABLE I. Elastic modes and relationship to elastic constants.

Mode <sup>a</sup>	Sample	Sample length $l_s$ (cm)	$\rho v^2$
$\vec{k}_{\text{long}} \parallel [100]$	02	0.939 42	$c_{11}$
$\vec{k}_{\text{long}} \parallel [001]$	01	1.0263	$c_{33}$
$\vec{k}_{\text{trans}} \parallel [001]$	01	1.0263	$c_{44}$
$\vec{k}_{\text{trans}} \parallel [110]$	01	1.0304	$c_{44}$
$\hat{e} \parallel [001]$			
$\vec{k}_{\text{trans}} \parallel [100]$	02	0.939 42	$c_{44}$
$\hat{e} \parallel [001]$			
$\vec{k}_{\text{trans}} \parallel [100]$	02	0.939 42	$c_{66}$
$\hat{e} \parallel [010]$			
$\vec{k}_{\text{trans}} \parallel [110]$	01	1.0304	$c' \equiv \frac{1}{2}(c_{11} - c_{12})$
$\hat{e} \parallel [1\bar{1}0]$			
$\vec{k}_{\text{long}} \parallel [110]$	01	1.0304	$c_L \equiv \frac{1}{2}(c_{11} + c_{12} + 2c_{66})$
$\vec{k}_{\text{trans}} \perp (011)$	02	1.0716	$c_T \equiv m^2 c_{66} + n^2 c_{44}$ <sup>b</sup>
$\hat{e} \parallel [100]$			
$\vec{k}_{\text{long}} \perp (011)$	02	1.0716	$c_{QL} = \frac{1}{2} \{ (c_{11}m^2 + c_{33}n^2 + c_{44}) + [(c_{11}m^2 - c_{33}n^2 + c_{44}(n^2 - m^2))^2 + 4m^2n^2(c_{13} + c_{44})^{1/2}]^{1/2} \}$ <sup>b</sup>
$\vec{k}_{\text{trans}} \perp (011)$			
$\hat{e} \perp [100]$	02	1.0716	$c_{QT} = \frac{1}{2} \{ (c_{11}m^2 + c_{33}n^2 + c_{44}) - [(c_{11}m^2 - c_{33}n^2 + c_{44}(n^2 - m^2))^2 + 4m^2n^2(c_{13} + c_{44})^{1/2}]^{1/2} \}$ <sup>b</sup>

<sup>a</sup> $\vec{k}_{\text{trans}}$  and  $\vec{k}_{\text{long}}$  are, respectively, the wave vectors associated with transverse and longitudinal propagation.  $\hat{e}$  is the polarization vector of the transverse modes.

<sup>b</sup> $(l, m, n)$  are the direction cosines of the wave vector with respect to the  $[100]$ ,  $[010]$ , and  $[001]$  axes, respectively. In  $\text{MnF}_2$  at  $T = 298$  K and for  $\vec{k} \perp (011)$  plane  $(l, m, n) = (0, 0.5619, 0.8272)$ .

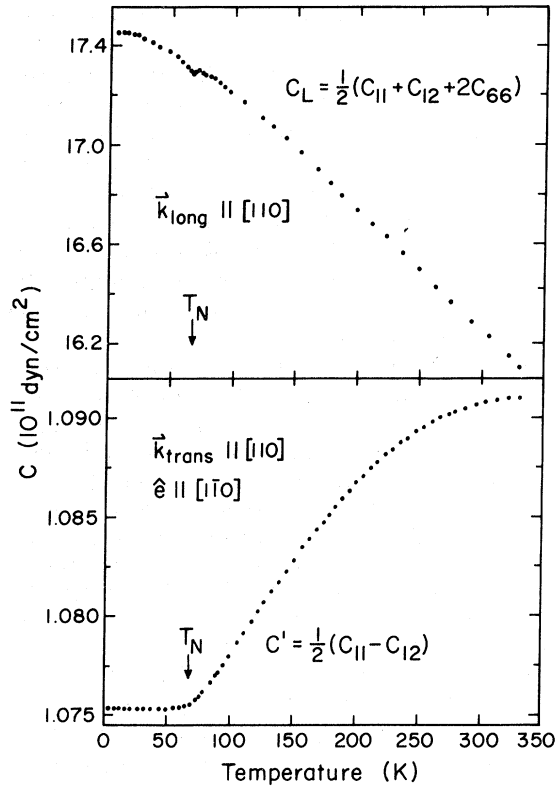


FIG. 2. Elastic constants  $c_{33}$  and  $c_{44}$  versus temperature,  $1.5 < T < 330$  K,  $\nu \approx 30$  MHz,  $\vec{k} \parallel [001]$ .

Table I) were identical to those obtained from propagation along the  $[001]$  axis and are not shown in Figs. 2 and 3.

#### IV. DISCUSSION

##### A. Theoretical Elastic Constants

Matossi<sup>10</sup> has proposed a model based on nearest-

neighbor interactions to describe the vibrational spectrum of materials with the rutile structure. He defined seven force constants between nearest-neighbor atoms (see Fig. 1) as follows:  $K_1$ , Mn-F atoms 2-5, etc.;  $K_2$ , Mn - F atoms 2-4, etc.,  $K'$ , F-F atoms 4-3, etc.;  $K''$ , F-F atoms 4-5, etc.;  $d_1$ ,  $d_2$ , and  $d_3$  are bond-bending forces at the Mn<sup>2+</sup> and F<sup>-</sup> sites. Using the assumptions that  $d_3 = 0$  and  $K' = K''$ , the Raman frequencies measured by Porto *et al.*<sup>15</sup> can be used to determine the constants  $K_1$ ,  $K_2$ , and  $K' = K''$ .  $K''$  and  $K_2$  are determined by the modes  $\omega_3(B_{1g}) = 61$  cm<sup>-1</sup> and  $\omega_5(E_g) = 271$  cm<sup>-1</sup>.  $K_1$  is then determined by either  $\omega_1(A_{1g}) = 341$  cm<sup>-1</sup> or  $\omega_4(B_{2g}) = 476$  cm<sup>-1</sup>. The value  $K_1$  used in the present calculation is the average of these two values. The force constants obtained in this way in units of  $10^5$  dyn/cm are  $K_1 = 1.03$ ,  $K_2 = 0.369$ ,  $K' = K'' = 0.0964$ . The ratio  $K_1/K_2 = 2.8 \pm 0.9$  indicates that the Mn - F bond between atoms 2 and 5 (Fig. 1) is significantly stronger than the Mn - F bond between atoms 2 and 4, although the interatomic distance is similar for both types of bonds.

The method outlined by Pandey<sup>11</sup> can be used to express the elastic free-energy density in terms of these force constants and one additional constant ( $K = -0.352 \times 10^5$  dyn/cm) describing the nearest-neighbor interaction between Mn<sup>2+</sup> ions along the  $c$  axis.<sup>24</sup> Comparing the coefficients of the strains in this expression with those of Eq. (1) results in relations between the force constants and the elastic constants  $c_{ij}$ . The theoretical elastic constants thus calculated are compared to the measured values at 300 K in Table III. The agreement between theory and experiment is rather good for the elastic constants  $c_{11}$ ,  $c_{33}$ ,  $c_{66}$ , and  $c_{12}$ . However, the calculated value for  $c_{44}$  is 22% high and that for  $c_{13}$  is 45% low. The lack of complete agree-

TABLE II. Summary of the elastic properties of MnF<sub>2</sub>.

Elastic constant <sup>a</sup>	Temperature (K)				Temperature coefficient at 300 K	
	300	200	100	4.2	Athermal <sup>b</sup>	( $10^{-6}$ K <sup>-1</sup> )
$c_{11}$	10.24	10.50	10.75	10.92	11.03	258
$c_{33}$	16.55	16.91	17.20	17.39	17.62	215
$c_{44}$	3.185	3.201	3.208	3.202	3.237	54.6
$c_{66}$	7.208	7.442	7.652	7.736	7.918	328
$c'$	1.091	1.087	1.078	1.075	...	...
$c_L$	16.25	16.73	17.20	17.45	17.70	297
$c_T$	4.439	4.519	4.588	4.609	4.679	181
$c_{QL}$	14.77	15.07	15.32	15.45	15.67	202
$c_{QT}$	2.985	3.031	3.070	3.130	3.127	158
$c_{12}$	7.95	8.20	8.47	8.64	...	...
$c_{13}$	7.07	7.26	7.44	7.46	...	...
$\Theta_D(E)$	259.7	260.6	261.2	261.6	...	...

<sup>a</sup>Values of the elastic constants are in units of  $10^{11}$  dyn/cm<sup>2</sup>.

<sup>b</sup>Athermal values are obtained by linear extrapolation of the limiting high-temperature behavior to  $T = 0$ .

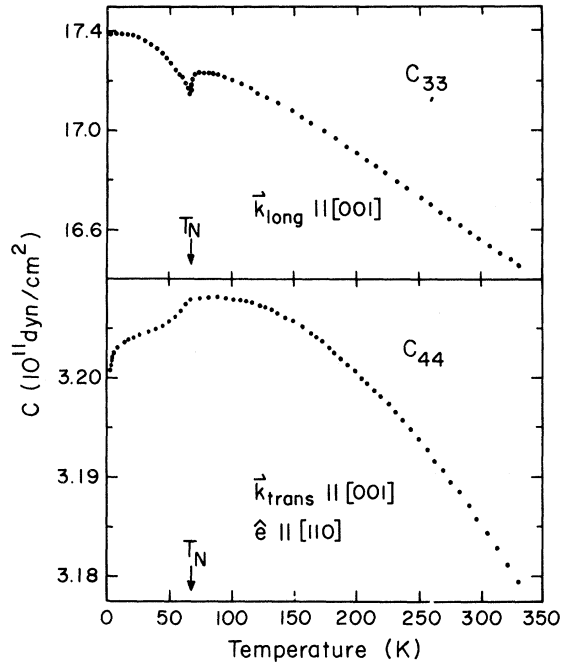


FIG. 3. Elastic constants  $c_L$  and  $c'$  versus temperature,  $4.2 < T < 330$  K,  $\nu \approx 30$  MHz,  $\vec{k} \parallel [110]$ .

ment is not unexpected, since the calculation can be criticized on several points. As has been pointed out by Porto *et al.*,<sup>15</sup> there exist inconsistencies in the Matossi model of up to 30% when attempts are made to predict the frequency of the optically inactive mode  $\omega_2(A_{2g})$  from the observed Raman frequencies. Determination of the force constant  $K_1$  from the individual Raman modes  $\omega_1(A_{1g})$  and  $\omega_4(B_{2g})$  results in values of  $0.70 \times 10^5$  dyn/cm and  $1.3 \times 10^5$  dyn/cm to be compared to the average value of  $1.03 \times 10^5$  dyn/cm used in the present calculation. Finally, the exclusion of other than nearest-neighbor forces is difficult to justify.

Recent work by Gubanov and Shur<sup>12</sup> and by Shur and Tsarev<sup>13</sup> on the vibrational spectrum of the rutile structure includes the effect of long-range Coulombic and dipolar forces. Unfortunately, data on the infrared active modes of the vibrational spectrum of  $\text{MnF}_2$  have not been reported.

#### B. Temperature Dependence

##### 1. Paramagnetic Region ( $T > T_N$ )

As seen in Figs. 2–5 for  $T \gtrsim \Theta_D(E)$ , the elastic constants associated with each mode [except  $c' = \frac{1}{2}(c_{11} - c_{12})$ ] decrease linearly with increasing temperature as expected from the very general thermodynamic theory of anharmonic lattices.<sup>21</sup> On the other hand, the mode  $c'$  shows quite different behavior (Fig. 3). The decrease in  $c'$  as the temperature is lowered ceases at  $T \approx T_N$ . However, it is difficult to explain this behavior on the

basis of the existence of magnetic order for  $T < T_N$ . It is known (see Secs. IV B 2 and IV B 3) that this mode couples to the magnetic modes via neither the linear magneto-elastic interaction nor the volume magnetostriction.

In Matossi's model the magnitude of  $c'$  is determined solely by the force constant  $K''$ . (This is readily seen from the expressions for the elastic constants in terms of the force constants.) On the other hand, the Raman mode  $\omega_3(B_{1g})$  is also completely determined by  $K''$ .<sup>10</sup> One might hope that the decrease in  $c'$  corresponds to a softening of  $\omega_3(B_{1g})$ . However,  $\omega_3(B_{1g})$  is found experimentally to increase from  $61 \text{ cm}^{-1}$  at  $T \approx 300$  K to  $\approx 71 \text{ cm}^{-1}$  for  $T \lesssim 20$  K.<sup>15</sup>

##### 2. Critical Region

Minima in the sound velocity and attenuation maxima in the neighborhood of magnetic phase transition are well documented effects.<sup>5</sup> The results of the present investigation are in qualitative agreement with the results of previous ultrasonic studies in the critical region of  $\text{MnF}_2$ .<sup>25,26</sup> In particular, the absence of minima in the transverse elastic constants leads to the conclusion that

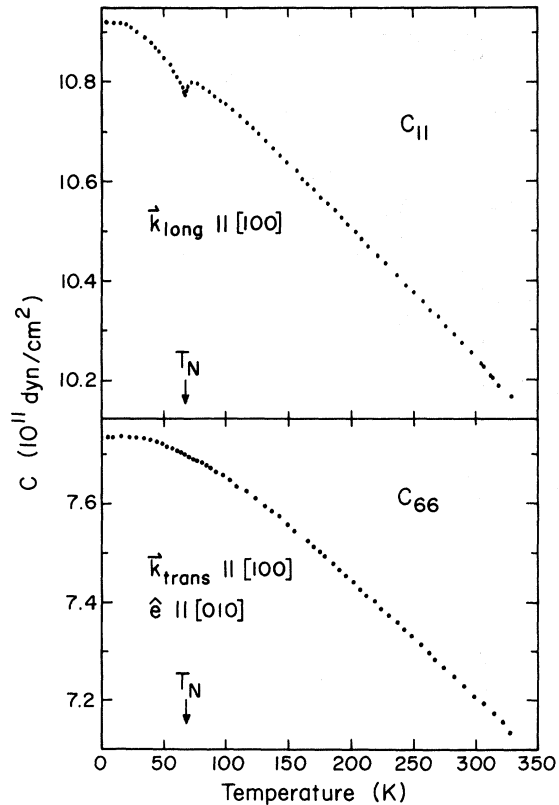


FIG. 4. Elastic constants  $c_{11}$  and  $c_{66}$  versus temperature,  $4.2 < T < 330$  K,  $\nu \approx 30$  MHz,  $\vec{k} \parallel [100]$ .

TABLE III. Comparison of theoretical and experimental elastic constants.

Elastic constant <sup>a</sup>	$c_{11}$	$c_{33}$	$c_{44}$	$c_{13}$	$c_{66}$	$c_{12}$
Theor	10.9	16.6	3.9	3.9	7.5	7.5
Expt	10.2	16.6	3.2	7.1	7.2	8.0
% diff	+7%	0	+22%	-45%	+4%	-6%

<sup>a</sup>The elastic constants are in units of  $10^{11}$  dyn/cm<sup>2</sup>.

the volume magnetostrictive spin-phonon interaction is responsible for the observed minima in the longitudinal modes. Comparison of the magnitude of the effect for the  $c_{33}$  mode with that for the  $c_{11}$  and  $c_L$  modes reveals an anisotropy of about a factor of 3.

### 3. Antiferromagnetic State

In the magnetically ordered state of the system ( $T < T_N$ ) the linear magneto-elastic (LME) interaction couples the elastic waves to the magnetic modes<sup>4</sup> producing an added contribution to the measured elastic constants:

$$c_{ij}^* = c_{ij} - \alpha_{ij} (2b^2/K). \quad (3)$$

$c_{ij}^*$  is the measured elastic constant,  $c_{ij}$  is the elastic constant in the absence of LME coupling,  $b$  is the LME coupling constant, and  $K$  is the mag-

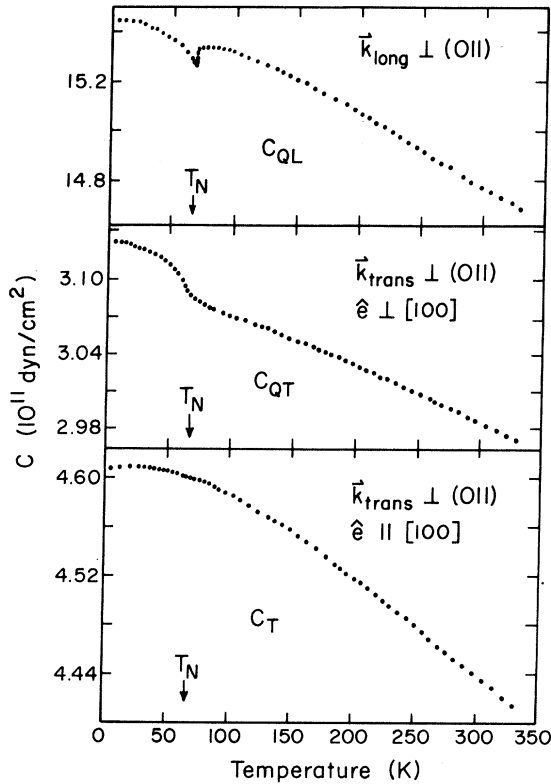


FIG. 5. Elastic constants  $c_{QL}$ ,  $c_{QT}$ , and  $c_T$  versus temperature,  $4.2 < T < 330$  K,  $\nu \approx 30$  MHz,  $\vec{k} \perp (011)$  plane.

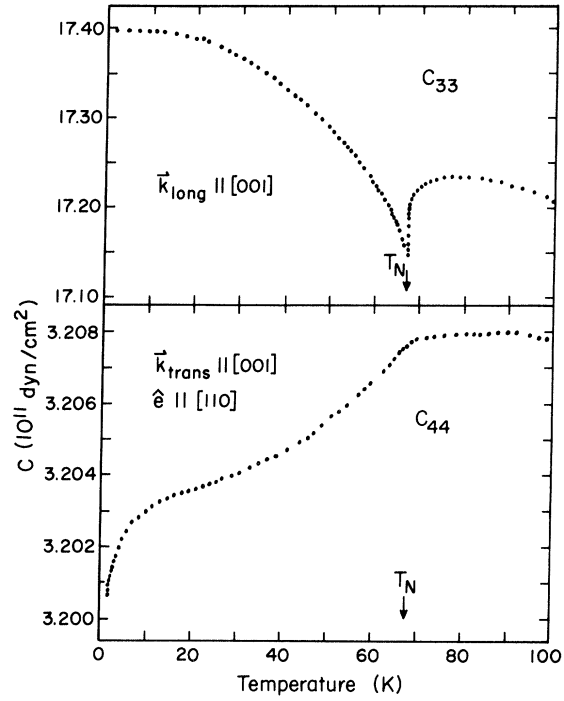


FIG. 6. Elastic constants  $c_{33}$  and  $c_{44}$  versus temperature,  $1.5 < T < 100$  K,  $\nu \approx 30$  MHz,  $\vec{k} \parallel [001]$ .

netic anisotropy constant. The assumption has been made that the LME interaction has uniaxial symmetry rather than the full tetragonal symmetry of the rutile structure (there is, therefore, only one coupling constant). This is a very good approximation for  $\text{MnF}_2$ . At  $T = 4.2$  K in  $\text{MnF}_2$ ,  $b = (5.4 \pm 0.5) \times 10^6$  erg/cm<sup>2</sup>, and  $K = 4.6 \times 10^6$  erg/cm<sup>3</sup>.<sup>4</sup> The coefficients  $\alpha_{ij}$  are zero for all the elastic modes described in Table I except  $c_{44}$ ,  $c_T$ ,  $c_{QL}$ , and  $c_{QT}$ . In an obvious notation one finds that  $\alpha_{44} = 1$ ,  $\alpha_T = n^2 = 0.683$ ,  $\alpha_{QL} = \frac{1}{2}(1 + \delta) = 0.766$ , and  $\alpha_{QT} = \frac{1}{2}(1 - \delta) = 0.234$ .  $\delta$  is defined by

$$\delta = \frac{[c_{44} + (c_{11}m^2 - c_{33}n^2)(n^2 - m^2) + 4m^2n^2c_{13}]}{[(c_{11}m^2 - c_{33}n^2 + c_{44}(n^2 - m^2))^2 + 4m^2n^2(c_{13} + c_{44})^2]^{1/2}}. \quad (4)$$

The temperature dependence of both  $b$  and  $K$  can be assumed to be roughly proportional to the square of the sublattice magnetization. Since  $\alpha_{ij} \lesssim 1$  and  $(2b^2/K)_{\text{max}} \approx 10^7$  dyn/cm<sup>2</sup>, the coupling term is expected to be observable only as it affects the temperature dependence of the elastic constants and then only in favorable circumstances.

Figures 2 and 6 clearly show an abrupt change in slope of elastic constant  $c_{44}^*$  versus  $T$ , for  $T$  just below  $T_N$  caused by the coupling term  $-(2b^2/K)$ . The sharp decrease in  $c_{44}^*$  at lower temperatures will be discussed below. The effect on  $c_{QL}^*$  is obscured by the minimum at  $T \approx T_N$  discussed in the Sec. IV B 2, while the effect on  $c_T^*$  is barely

perceptible. On the other hand,  $c_{QT}^*$  unexpectedly shows a positive increase at  $T \approx T_N$ , which cannot be explained by the LME theory. The behavior of  $c_{QT}^*$  is quite similar to that observed for the  $c_{44}$  mode in cubic  $\text{RbMnF}_3$ ,<sup>2</sup> but is not at present understood.

Somewhat more surprising is the decrease in  $c_{44}$  (approximately proportional to  $T^{-1}$ ) as the temperature is lowered further (see Figs. 2 and 6). The LME theory is incapable of explaining this phenomenon; for  $T \ll T_N$ , both  $b$  and  $K$  are essentially independent of temperature. Similarly, for  $T \ll \Theta_D$  the  $c_{ij}$  themselves must be temperature independent.

Since the only physical quantity in the material which has a  $T^{-1}$  temperature dependence at low temperatures is the nuclear-spin susceptibility, it is tempting to attribute the effect to a coupling of the elastic mode to either the  $\text{Mn}^{55}$  or  $\text{F}^{19}$  spin systems. It can be shown<sup>27</sup> that the magnon-coupled nuclear spin-phonon interaction<sup>28</sup> will make a contribution to  $c_{44}^*$  of the form

$$-2(AbM_0/K)^2 \chi_N(T) [\omega^2/(\omega_0^2 - \omega^2)], \quad (5)$$

where  $A$  is the hyperfine constant,  $M_0$  is the electronic sublattice magnetization,  $\chi_N(T) \sim T^{-1}$  is

the nuclear-spin susceptibility,  $\omega$  is the frequency, and  $\omega_0$  is the nuclear Larmor frequency as determined by the hyperfine field. Of the modes propagating along symmetry axes of the crystal only  $c_{44}$  will be coupled to the nuclei. However, order-of-magnitude estimates indicate that this contribution is 6–8 orders of magnitude too small to account for the experimentally observed behavior of  $c_{44}^*$ . Other types of coupling mechanisms can be estimated to be much weaker still.

Another possible explanation is that the phenomenon results from the relaxation of anelastic defects.<sup>29</sup> This possibility is difficult to eliminate but it should be noted that there is no defect whose symmetry is allowed by the rutile structure which would couple to only the  $c_{44}$  mode. The coupling to other modes, however, may be very weak for reasons other than those based on symmetry alone.

Experiments are presently being carried out at lower temperatures and at higher frequencies with the hope that these measurements will result in some insight into the origin of this interesting effect.

*Note added in proof.* Henderson, Meyer, and Guggenheim (private communication) have recently found a low-temperature calorimetric Debye temperature of  $255 \pm 3$  K in  $\text{MnS}_2$ .

<sup>†</sup>Work supported by Advanced Research Projects Agency through the Materials Science Center at Cornell University, MSC Report No. 1309.

\*Present Address: IBM, Thomas J. Watson Research Center, Yorktown Heights, N. Y. 10598.

<sup>1</sup>D. I. Bolef and J. DeKlerk, Phys. Rev. **129**, 1063 (1963).

<sup>2</sup>R. L. Melcher and D. I. Bolef, Phys. Rev. **178**, 864 (1969).

<sup>3</sup>R. L. Melcher and D. I. Bolef, Phys. Rev. **186**, 491 (1969).

<sup>4</sup>R. L. Melcher, J. Appl. Phys. **41**, 1412 (1970).

<sup>5</sup>For a review of elastic phenomena associated with second-order magnetic phase transitions and a complete bibliography see B. Luthi, T. J. Moran, and R. J. Pollina, J. Phys. Chem. Solids (to be published).

<sup>6</sup>Y. Shapira, S. Foner, and A. Missetich, Phys. Rev. Letters **23**, 98 (1969).

<sup>7</sup>R. L. Melcher and D. I. Bolef, Phys. Rev. **184**, 556 (1969).

<sup>8</sup>J. B. Merry and D. I. Bolef, Phys. Rev. Letters **23**, 274 (1969).

<sup>9</sup>M. Griffel and J. W. Stout, J. Am. Chem. Soc. **72**, 4351 (1950).

<sup>10</sup>F. Matossi, J. Chem. Phys. **19**, 1543 (1951).

<sup>11</sup>H. N. Pandey, Phys. Status Solidi **11**, 743 (1965).

<sup>12</sup>A. I. Gubanov and M. S. Shur, Fiz. Tverd. Tela **7**, 2626 (1965) [Soviet Phys. Solid State **7**, 2124 (1966)].

<sup>13</sup>M. S. Shur and Yu. N. Tsarev, Fiz. Tverd. Tela [Soviet Phys. Solid State **10**, 2293 (1969)].

<sup>14</sup>A. S. Barker, Jr., Phys. Rev. **136**, A1290 (1964).

<sup>15</sup>S. P. S. Porto, P. A. Fleury, and T. C. Damen, Phys. Rev. **154**, 522 (1967).

<sup>16</sup>K. S. Aleksandrov, L. A. Shabanova, and V. I.

Zinenko, Phys. Status Solidi **33**, K1 (1969).

<sup>17</sup>The samples were obtained from Optovac, Inc., North Brookfield, Mass.

<sup>18</sup>R. L. Melcher, D. I. Bolef, and J. B. Merry, Rev. Sci. Instr. **39**, 1618 (1968).

<sup>19</sup>D. F. Gibbons, Phys. Rev. **115**, 1194 (1959).

<sup>20</sup>G. A. Alers and J. R. Neighbors, J. Appl. Phys. **28**, 1514 (1957).

<sup>21</sup>For a discussion of anharmonic effects in solids see G. Leibfried and W. Ludwig, in *Solid State Physics*, edited by F. Seitz and D. Turnbull (Academic, New York, 1961), Vol. 12.

<sup>22</sup>D. D. Betts, A. B. Bhatia, and G. K. Horton, Phys. Rev. **104**, 43 (1956); see also G. A. Alers, *Physical Acoustics*, edited by W. P. Mason (Academic, New York, 1965), Vol. III B.

<sup>23</sup>E. Catalano and N. E. Phillips, J. Phys. Soc. Japan Suppl. **17**, B-1, 527 (1962).

<sup>24</sup>Reference 11, Eq. (5) is incorrect as written. In the notation of Ref. 11 the correct expression is

$$U = \frac{1}{2} K_1 [\Delta r_{1,2}^2 + \Delta r_{1,3}^2 + \Delta r_{10,14}^2 + \Delta r_{10,16}^2] \\ + K [\Delta r_{1,4}^2 + \Delta r_{1,5}^2 + \Delta r_{10,2}^2 + \Delta r_{10,12}^2] \\ + \frac{1}{2} K' [\Delta r_{2,12}^2 + \Delta r_{4,6}^2] + K'' [\Delta r_{2,4}^2 + \Delta r_{2,5}^2 + \Delta r_{2,6}^2 + \Delta r_{2,7}^2 \\ + \Delta r_{2,13}^2 + \Delta r_{2,14}^2 + \Delta r_{2,15}^2 + \Delta r_{2,16}^2] + \frac{1}{2} K [\Delta r_{1,8}^2 + \Delta r_{1,9}^2].$$

<sup>25</sup>R. G. Leisure and R. W. Moss, Bull. Am. Phys. Soc. **14**, 835 (1969); Phys. Rev. **188**, 840 (1969).

<sup>26</sup>A. Ikushima, Phys. Letters **29A**, 364 (1969); J. Phys. Chem. Solids **31**, 283 (1970).

<sup>27</sup>R. L. Melcher, Phys. Rev. B **1**, 4496 (1970).

<sup>28</sup>S. D. Silverstein, Phys. Rev. **132**, 997 (1963).

<sup>29</sup>A. S. Nowick and W. R. Heller, Advan. Phys. **14**, 101 (1965).